SPANDIDOS PUBLICATIONS

VP-16 (etoposide) and calphostin C trigger different nuclear but akin cytoplasmic patterns of changes in the distribution and activity of protein kinase C-ß$_I$ in polyomavirus-transformed pyF111 rat fibroblasts

ANNA CHIARINI[1], JAMES F. WHITFIELD[2], UBALDO ARMATO[1] and ILARIA DAL PRA[1]

[1]Histology and Embryology Unit, Department of Biomedical and Surgical Sciences, University of Verona Medical School, Verona I-37134, Italy; [2]Institute for Biological Sciences, National Research Council of Canada, Ottawa, Ontario K1A 0R6, Canada

Received August 24, 2005; Accepted October 3, 2005

Abstract. Protein kinase C (PKC) isoforms regulate cell proliferation and apoptosis. Since the PKC isoenzyme complement varies considerably from cell type to cell type, a PKC's responsiveness to an apoptogenic challenge must be defined for both the type of apoptogen and the type of cell. We have already reported that the changes in the distribution and activity of PKC-δ in apoptosing polyomavirus-infected/transformed Fischer rat embryo pyF111 fibroblasts depend on the type of apoptogen. Here, we show that this is also true for PKC-ß$_I$ in pyF111 cells treated with the slow DNA-damaging VP-16 (etoposide) or the fast-acting (in the cytoplasm) calphostin C. These apoptogens caused quite different shifts of the PKC-ß$_I$ level and activity in the nuclear membrane (NM) and nucleoplasm (NP), but corresponding changes in the cytosol (CS) and cytoplasmic particulate (CP) fractions. The hefty translocation of PKC-ß$_I$ onto the CP fraction and its increased activity there suggest the possible triggering of a cytochrome *c*/caspase-mediated apoptosis-inducing mechanism common to both agents. The present results are a necessary lead-up to functional proteomic analyses aimed at identifying the molecules forming the local PKC-ß$_I$ signalling modules under different conditions.

Correspondence to: Professor Ubaldo Armato, Histology and Embryology Unit, Department of Biomedical and Surgical Sciences, University of Verona Medical School, Strada Le Grazie 8, Verona I-37134, Italy
E-mail: ubaldo.armato@univr.it

Abbreviations: AO, acridine orange; CF, carboxy-terminal (catalytic) fragment of PKC; CS (or SN2), cytoplasmic soluble fraction (cytosol); EB, ethidium bromide; N (or P1), total nuclear fraction; NM, nuclear envelope-enriched fraction; NP, nucleoplasmic fraction; PKC, protein kinase C; SN1, whole cytoplasmic fraction; VP-16, etoposide

Key words: protein kinase C-ß$_I$, apoptosis, etoposide (VP-16), calphostin C, subcellular fractions, pyF111 cells

Introduction

The expression and intracellular distribution of the several PKC isoforms depend on the functional needs of a particular cell or tissue and its responsiveness to external stimuli (1,2). Because of a common catalytic domain they can catalyze the phosphorylation of similar substrates, but it is their membership in variously sited signalling complexes with different components in diverse types of cells that gives them their functional variety (1,2). PKC's signalling is involved in many cellular functions including proliferation and apoptosis (2,3). Given the large number of PKC isoforms and their rather small differences, trying to identify their role(s) in any common cell function such as proliferation is a challenging task because of conflicting results from various cell models from diverse species.

PKC-ß$_I$ and PKC-ß$_{II}$ are the products of alternatively spliced transcripts of the same gene that differ by only 50 amino acids at their C-tails (4). PKC-ß$_I$ activation requires transphosphorylations by Btk (Bruton's tyrosine kinase) and Syk protein tyrosine kinases (5) as well as autophosphorylations (6). Site-directed mutagenesis of the autophosphorylation sites (Thr^{635}/Thr^{642}) on the C-tail of PKC-ß$_I$ affects both the enzyme function and subcellular localization (6). PKC-ß$_I$ is 10 times more sensitive to Ca^{2+} than PKC-ß$_{II}$ (7), but the two 'siblings' are similarly sensitive to diacylglycerols (DAGs) (8). Both PKC-ßs are involved in cell growth and apoptosis (9). Various stimuli can induce PKC-ß$_I$ to migrate to the nucleus (and nucleus-associated insoluble structures) followed by intra-nuclear proteolysis of its holoprotein in epithelial cells (10) as well as BALB/c 3T3 and C3H10T1/2C 18 mouse fibroblasts (11). Depending on the cell type, PKC-ß$_I$ in various normal and transformed cell types can be involved in stimulating proliferation often with loss of differentiation (10,12-15), or inhibiting proliferation with a stimulation of

differentiation (16-19). Also, depending on the type of cell PKC-ßI may counteract (20,21), or be the effector (22-24) of the actions of various apoptogenic agents.

In previous experiments to define the role(s) of the several PKC isoenzymes in apoptosis, we used polyomavirus-infected/transformed pyF111 Fischer rat embryo fibroblasts because they are hypersusceptible to apoptogenesis. This hypersusceptibility is due to the cells making the pro-apoptotic mitochondrial pore-forming Bax protein, but not the anti-apoptogenic Bax-blocking Bcl-2 and Bcl-X_L proteins (25-28). We found that the slow-onset apoptogenesis triggered by topoisomerase-II inhibitors like etoposide (VP-16) (29) and the rapid-onset apoptogenesis triggered by the PKC and phospholipase inhibitor calphostin C (30) caused different changes in the intranuclear distribution and specific activity of PKC-δ, although they both increased the amount and activity of cytoplasmic particulate (CP)-bound PKC-δ holoenzyme (26,27). Then, we turned our attention to the PKC-ß 'siblings'. Since the two isoenzymes are structurally similar, they would be expected to respond likewise to apoptogens (16). They both move to the nuclei of apoptosing pyF111 cells, but they perform different tasks when they get there. In VP-16-treated cells PKC-ßII, but not PKC-ßI, is an apoptotic lamin kinase that forms a large complex in the nuclear membrane with lamin B1 as well as the caspase 6 protease, which by destroying the phosphorylated lamin disrupts nuclear structure and function (28). Hence, we have begun searching for clues to any role(s) PKC-ßI might have in apoptosis by studying the intracellular movements of enzymes in apoptosing pyF111 cells. We show that VP-16 and calphostin C do indeed affect differently the nuclear membrane and nucleoplasmic distribution and specific activity of PKC-ßI just as they do for PKC-ßII and PKC-δ (26-28), but they cause (though with obvious different timings) similar PKC-ßI-related changes in the cytosolic and cytoplasmic particulate fractions.

Materials and methods

Cell cultures. Polyomavirus-infected/transformed pyF111 Fischer rat embryo fibroblasts were cultured and handled as previously detailed (26-28).

Apoptosis induction and detection. Experiments were started by planting $1.2x10^6$ cells in each of several F-160 flasks. Twenty-four hours later (i.e. at the experimental '0-h'), the cells in some flasks were sampled ('0-time' controls), the medium in some other flasks was replaced with the same, but fresh, medium (control group), while the medium in the remaining flasks was replaced by fresh medium containing either the topoisomerase-II inhibitor VP-16 [etoposide or 4*N*-demethyl-epipodophyllotoxin 4-(4,6-*O*-ethylidene-ß-D-glucopyranoside) 1.0 μg ml^{-1} (29)] or calphostin C (UCN-1028C; 75 nM) (both from Sigma Chemical Co., St. Louis, MO), a perilenequinone metabolite of the fungus *Cladosporium cladosporioides* reported to inhibit PKC (and phospholipase) activity by competing with diacylglycerol and phorbol esters for binding to the enzyme's C1 regulatory domain (30). After being added to the culture growth medium ('0-h'), calphostin C was activated by illumination for 0.5 h with ordinary fluorescent light (apoptosis group) and incubated in the dark. Control cultures without calphostin C in their medium were also illuminated. The medium was not changed again during observation periods that ranged from 6 to 72 h for the VP-16-treated group and from 15 min to 4.5 h for the calphostin C-exposed group, whose medium after the illumination contained photoactivated calphostin C. Cell viability was assessed by means of epifluorescence microscopy according to Amarante-Mendez *et al* (31), using a solution ($1:1^{v/v}$) of acridine orange (AO; 0.1 mg ml^{-1} in PBS; filter setting for FITC) and ethidium bromide (EB; 0.1 mg ml^{-1} in PBS; specific filter setting for rhodamine) (both from Molecular Probes, Inc., Eugene, OR).

Subcellular fractionation. Cells were harvested by scraping them into cold PBS and then centrifuging the suspension at 200 x g for 10 min. The sedimented cells were carefully resuspended in a solution containing 10 mM Hepes, pH 7.9, 10 mM KCl, 1.0 mM $MgCl_2$, 1.0 mM DTT, 20 μM sodium orthovanadate, and a complete EDTA-free protease inhibitor cocktail (Roche Diagnostics S.p.A., Milan, Italy), chilled on ice for 15 min, and gently lysed by adding $0.6\%^{v/v}$ Nonidet P40. The lysate was spun down at 200 x g for 10 min to produce the *P1* (or *N*) pellet, containing the nuclei, and the *SN1* supernatant. The *P1* fraction was quickly suspended in a large volume of hypotonic buffer (10 mM Tris pH 7.4, 10 mM Na_2HPO_4, 1.0 mM DTT, 20 μM sodium orthovanadate, and a complete EDTA-free protease inhibitor cocktail (Roche Diagnostics S.p.A.), containing DNase I and heparin (0.2 and 5 mg/mg of nuclear protein, respectively). This suspension was incubated at 4°C for 45 min, and then centrifuged at 9500 x g for 15 min. The resulting pellet was the nuclear membrane-enriched *NM* fraction, and the supernatant was the nucleoplasmic *NP* fraction. The *SN1* supernatant was centrifuged at 100,000 x g for 1 h. It yielded the *SN2* supernatant or cytosolic fraction *(CS)*, and the *P2* pellet or cytoplasmic particulate fraction *(CP)*. The purities of these various fractions were assessed from their contents of the cytosolic marker lactate dehydrogenase (E.C. 1.1.1.27) measured by the method of McIntosh and Plummer (32), the plasma membrane marker 5'-nucleotidase (E.C.3. 1.3.5) measured by the method of Ipata as modified by McIntosh and Plummer (32), and the nuclear marker lamin B assessed by Western immunoblotting (26,28).

Western immunoblotting. The protein contents of the subcellular fractions were assayed by the Bradford method (33). Western immunoblots were prepared as previously described (26-28). To immunodetect PKC-ßI, the blots were probed with a rabbit IgG polyclonal antibody that recognized its specific carboxy-terminal sequences (final dilution 1.0 μg ml^{-1}; Santa Cruz Biotechnology, Inc., Santa Cruz, CA). All the PKC-ßI-specific staining could be suppressed by adding the peptide against the antibody it was raised (Santa Cruz Biotechnology, Inc.). Some blots were also probed with mouse polyclonal antibody (final dilution: 1.0 μg ml^{-1}) to detect lamin B1. Blots were next incubated with alkaline phosphatase-conjugated anti-rabbit IgG (Santa Cruz Biotechnology, Inc.), and stained with BCTP/NBT liquid substrate reagent (Sigma). Pictures of the specific bands in the developed blots, taken with an Olympus Camedia C-3030™ digital camera, were

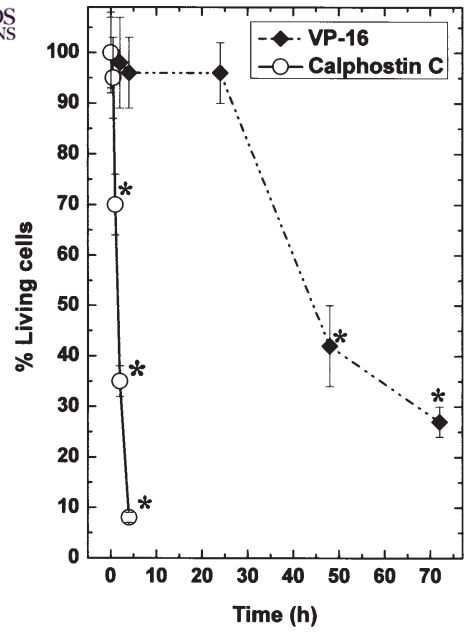

Figure 1. The timings of VP-16- and calphostin C-induced apoptosis are very different in pyF111 rat fibroblasts. Cells were treated with either 1.0 μg ml^{-1} VP-16 or 75 nM calphostin C, sampled at devised time points, stained with the AO+EB mixture, and counted under the fluorescence microscope as detailed in Materials and methods. Each point on the curves is the mean value ±1 SEM of five separate experiments. *p<0.05 with respect to corresponding 0-h values.

densitometrically analyzed using Sigmagel™ software (Jandel Corp., Erkrath, Germany).

Immunoprecipitation of PKC-β_I. The same amount of protein from each subcellular fraction was used for immunoprecipitation experiments. The protein was incubated at 4˚C for 3 h with the anti-PKC-β_I antibody (Santa Cruz Biotechnology, Inc.) conjugated to Immunopure® immobilized protein A (Pierce Chemical Co., Rockford, IL). The immunocomplex-bearing beads were collected by centrifugation at 2500 rpm for 5 min at 4˚C, and washed 5 times with TBS (20 mM Tris pH 7.4, 200 mM NaCl), 1.0 mM DTT, 20 μM sodium orthovanadate, and complete EDTA-free protease inhibitor cocktail (Roche Diagnostics S.p.A.). After a final wash, the immunocomplex-bearing beads were resuspended in TBS and their PKC-β_I-specific activity assayed.

Assay of immunopurified native and calcium-stimulated PKC-β_I activities. A colorimetric PKC assay kit, the Spinzyme Format™ (Pierce Chemical Co.) including the ε-peptide as a colorimetric substrate was used to selectively measure PKC-β_I native activities immunoprecipitated from the various subcellular fractions (26-28). PKC-β_I activities were also tested after adding exogenous calcium (0.5 mM) to the same assay mixtures. The results were expressed in arbitrary units calculated for each sample as the ratios between optical density values and micrograms of the immunoprecipitated protein.

Statistical analysis. Statistical significance was assessed by one-way ANOVA test with Bonferroni's *post hoc* multiple comparison test: only differences with p<0.05 were regarded as significant.

Results

Apoptosis induction in pyF111 cells. The numbers of substrate-adhering cells in untreated pyF111 cultures increased 10-fold between '0' h (i.e., 24 h after planting in flasks and a fresh medium change at 24 h) and 72 h when >99.7% of the cells were still viable (data not shown) (25). The responses of pyF111 cells to VP-16 and calphostin C have been previously described (26-28). Briefly, VP-16 (1.0 μg ml^{-1}) immediately stopped the fibroblasts proliferating by inhibiting the topoisomerase II activity needed to progress through mitosis (28,29). Apoptogenesis started 24 h later and by 48 h 58% of the cells were dead, and by 72 h 73% were dead (Fig. 1). By contrast, exposure to calphostin C (75 nM), both during and after its 30-min photoactivation, had induced apoptosis in 30% of the cells after 1.25 h. By 2.5 h 65% of the cells were dead and by 4.5 h 93% were dead (Fig. 1).

Apoptotic changes in PKC-β_I subcellular distribution and activity.

NM (nuclear membrane) fraction. At '0'-time there was abundant 80-kDa PKC-β_I holoenzyme in the lamin B-enriched NM fraction, but there were few 47-kDa carboxy-terminal (CF)-β_I fragments (Fig. 2A and B). The 0-h immunoprecipitable native PKC-β_I activity in the NM was not increased by adding exogenous calcium (0.5 mM) to the assay mixtures, indicating that untreated cells had virtually no calcium-activatable PKC-β_I molecules in their nuclear envelopes (Fig. 2A and B).

VP-16. After a -35% (p<0.05) drop during the first 24 h, the amount of PKC-β_I holoenzyme in the NM started accumulating and had more than doubled (p<0.001) by 72 h with respect to 24 h (Fig. 2A). The holoenzyme cleavage stopped and the 47-kDa CF-β_I fragments disappeared between 0 and 24 h. However, cleavage resumed and the CF level rose by >40% (p<0.02) vs. the 0-time levels along with the accumulating holoenzyme between 24 and 48 h and then plateaued (Fig. 2A). The immunoprecipitable PKC-β_I native activity in the NM doubled by 24 h and trebled by 48 h (in both cases, p<0.001), reaching a 3.3-fold level by 72 h (p<0.001 vs. 0-h values) (Fig. 2A). Adding calcium (0.5 mM) to the assay mixture at 24 h did not affect the kinase activity, but adding it at 48 and 72 h further increased by 1.5 times (p<0.001 at either time point), i.e. five-fold its 0-h level the PKC-β_I activity in the NM (Fig. 2A). Therefore, a significant fraction of the PKC-β_I molecules that accumulated in the nuclear envelope after 24 h could be activated by Ca^{2+} (Fig. 2A).

Unlike the closely related PKC-β_{II} in apoptosing VP-16-treated pyF111cells (28), the PKC-β_I moving into the nuclear membrane along with it did not complex with lamin B1 and, therefore, did not co-immunoprecipitate with the lamin B1 from the NM fractions of VP-16- or calphostin C-treated cells (not shown).

Calphostin C. In contrast to the accumulation of PKC-β_I in the NM of VP-16-treated cells occurring after 24 h (Fig. 2A),

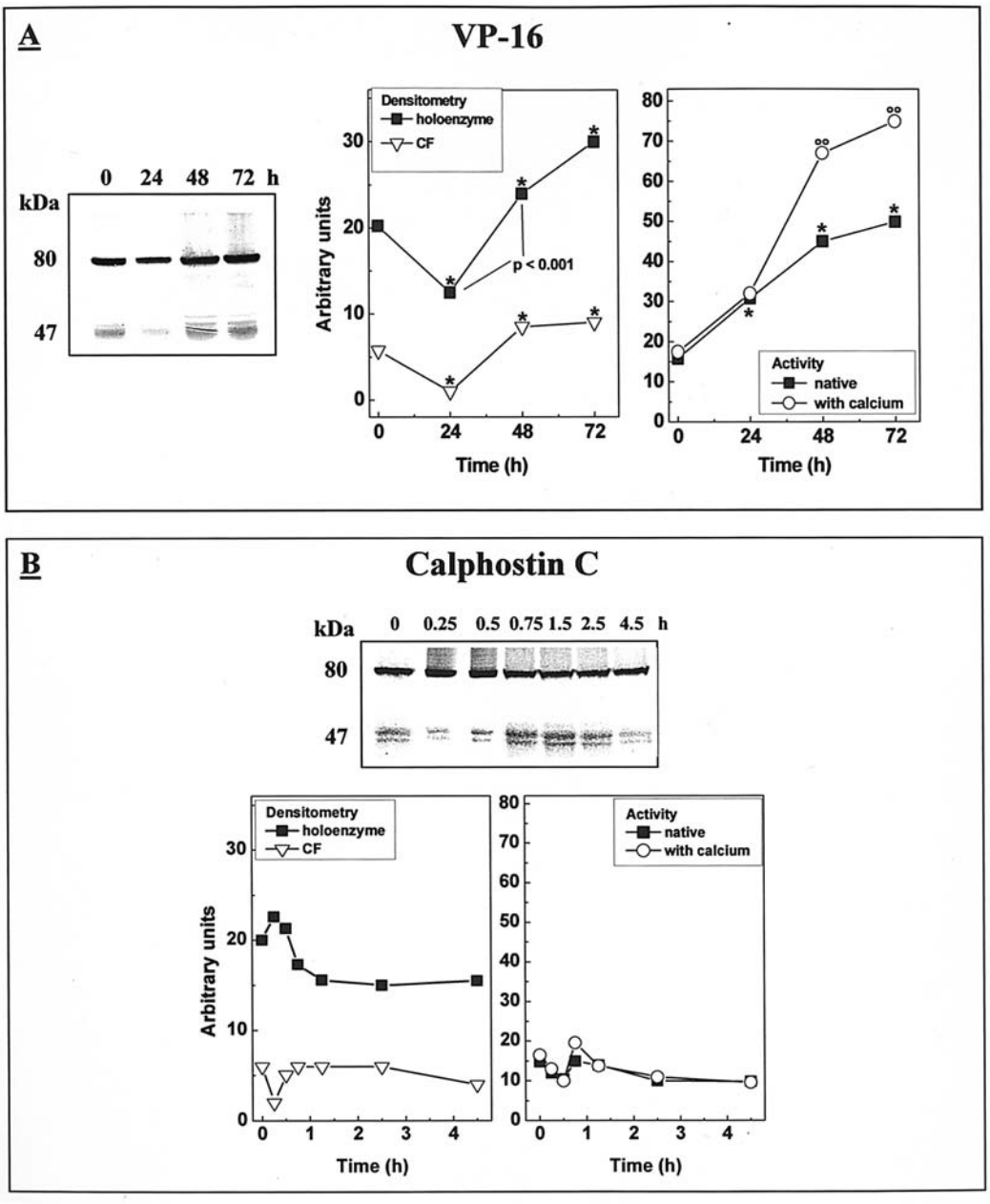

Figure 2. Nuclear membrane (NM) fraction. The distinct effects of VP-16 (A) and calphostin C (B) on the levels of PKC-ß$_I$ holoenzyme, 47-kDa carboxy-terminal (catalytic) fragment (CF), and immunoprecipitable activities in the NM (nuclear envelope) fraction of pyF111 cells. Cells were treated with either 1.0 μg ml^{-1} VP-16 or 75 nM calphostin C, sampled, and their NM fraction isolated; immunoblots were set up and activity assays performed with NM fractions as detailed in Materials and methods. The immunoblots and the points on the densitometric and specific activity curves are representative of at least four separate experiments carried out with each apoptogen in triplicate. The bands of the 80-kDa PKC-ß$_I$ holoenzyme and its 47-kDa CF were visualized by an antibody directed against a ß$_I$-specific amino acid sequence in the enzyme's C-terminus. SEMs, not shown, were within ±12% of the corresponding mean values. The indication 'with calcium' means that PKC-ß$_I$-activity was also measured after adding exogenous calcium (0.5 mM) to the assay mixtures in which native activity had been assessed. *p<0.001 with respect to related 0-h values; °°, p<0.001 with respect to values of corresponding time points.

the levels of PKC-ß$_I$ holoenzyme and its 47 kDa CF-ß$_I$ fragment did rise and fall slightly yet not significantly between 0 and 4.5 h (Fig. 2B). The immunoprecipitable PKC-ß$_I$ native kinase activity exhibited marginal fluctuations prior to a slow decrease from 45 min onwards as the cells were dying (Fig. 2B). There was no appreciable appearance of a Ca^{2+}-activatable PKC-ß$_I$ pool in the NM as there was in the VP-16-treated cells (Fig. 2A and B).

NP (nucleoplasm) fraction. A significant amount of PKC-ß$_I$ holoenzyme, but not its CF-ß$_I$ fragment, was initially detectable in the NP fraction of pyF111 cells, where it was associated with the highest levels of native activity of all fractions. This activity was slightly (+19%) but not significantly increased by adding Ca^{2+} to the assay mixtures (Fig. 3A and B).

VP-16. The amount of PKC-ß$_I$ holoenzyme remained steady for 24 h and then began slowly falling to 74% (p not significant) of the starting value by 72 h (Fig. 3A). Conversely, the immunoprecipitable native activity, which had dropped an insignificant 23% by 24 h, doubled (p<0.001) within the next 24 h, and then dropped (Fig. 3A). Adding calcium to the assay mixture increased the activity levels (24 h: +55%,

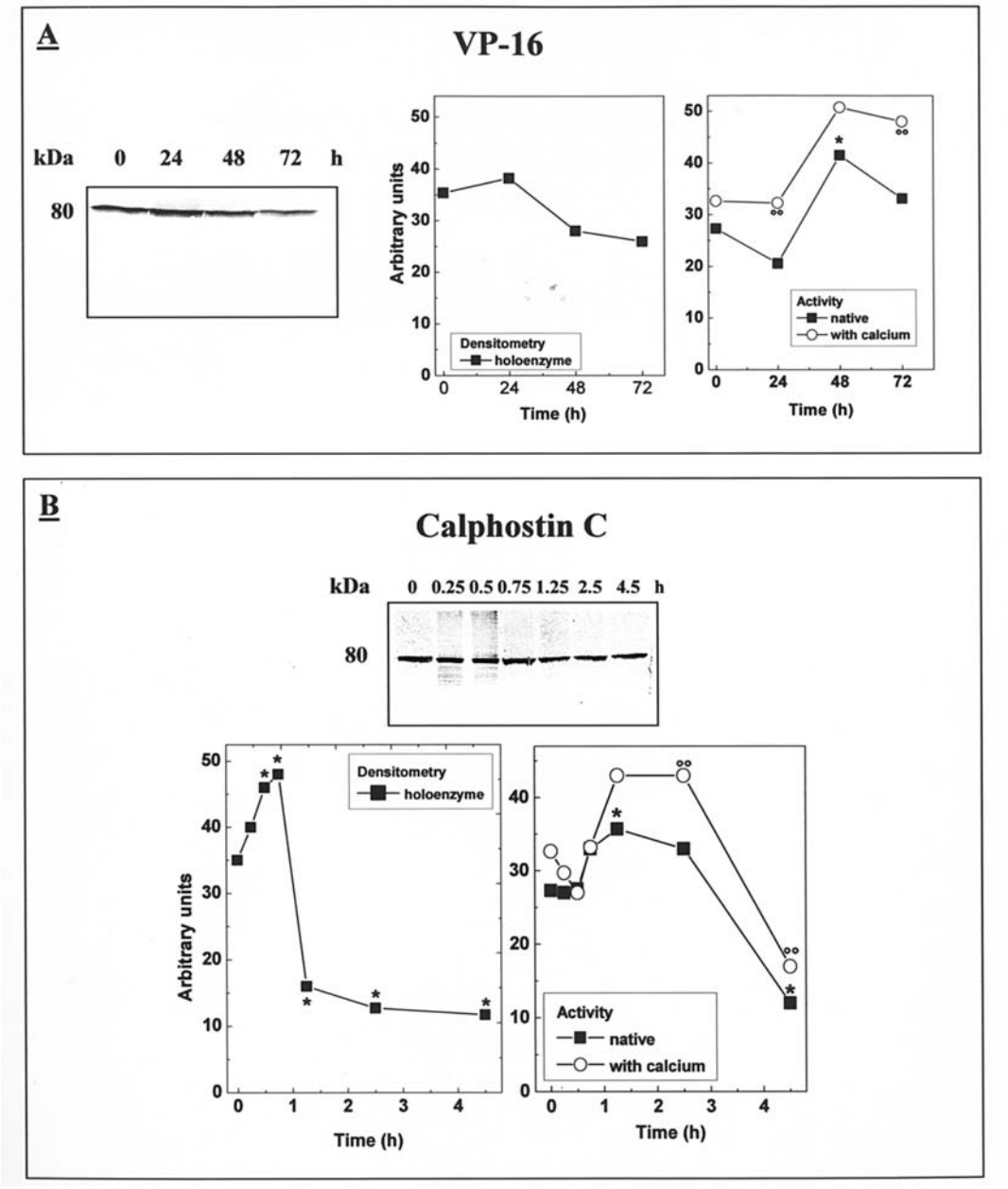

Figure 3. Nucleoplasmic (NP) fraction. The divers effects of VP-16 (A) and calphostin C (B) on the distribution and activity levels of PKC-ß$_I$ in the NP (nucleoplasm) fraction of pyF111 cells. Cells were treated with either 1.0 μg ml^{-1} VP-16 or 75 nM calphostin C, sampled, and their NP fraction isolated; other experimental procedures were as indicated for Fig. 2. The representative immunoblots and the points on the densitometric and specific activity curves are from at least four separate experiments carried out with each apoptogen in triplicate. SEMs, not shown, were within ±13% the corresponding mean values. *p<0.05 with respect to 0-h values; °°, p<0.05 with respect to values of corresponding time points.

p<0.01; 48 h: +20%, p not significant; and +47%, p<0.01 vs. the native values of corresponding time points) (Fig. 3A).

Calphostin C. The holoenzyme rose by 40% (p<0.02) between 0 and 45 min but then dropped sharply to only about 44% of the starting level (p<0.01) by 1.25 h to plateau thereafter (Fig. 3B). The native PKC-ß$_I$ activity did not change during the first 30 min but, despite the post-illumination presence of activated calphostin C, then rose 32% (p<0.05) between 30 and 1.25 h, stayed close to that level until 2.5 h, and then dropped by 63% (p<0.001) between 2.5 and 4.5 h (Fig. 3B). Calcium further increased the PKC-ß$_I$ activity by 20 (p not significant), 32 (p<0.05), and 44% (p<0.02) when added to the assay mixture at 1.25, 2.5, and 4.5 h, respectively (Fig. 3B).

Hence, a Ca^{2+}-activatable pool of PKC-ß$_I$ holoenzyme was maintained in the NP fractions of calphostin C-treated cells as well as in the NP fractions of untreated and VP-16-treated cells (Fig. 3A and B).

CS (cytosolic) fraction. The PKC-ß$_I$ holoenzyme, but not its CFs, existed in the untreated CS fractions of pyF111 cells, where it was associated with a rather low level of immunoprecipitable native activity that was not significantly affected by adding Ca^{2+} to the assay mixture (Fig. 4A and B).

VP-16. The holoenzyme levels progressively declined (24 h: -23%, p not significant; 48 h: -34%, p<0.05; 72 h: -47%, p<0.02), while its native activity did not change between 0 and 24 h, but increased (+45%, p<0.02) between 24 and 48 h,

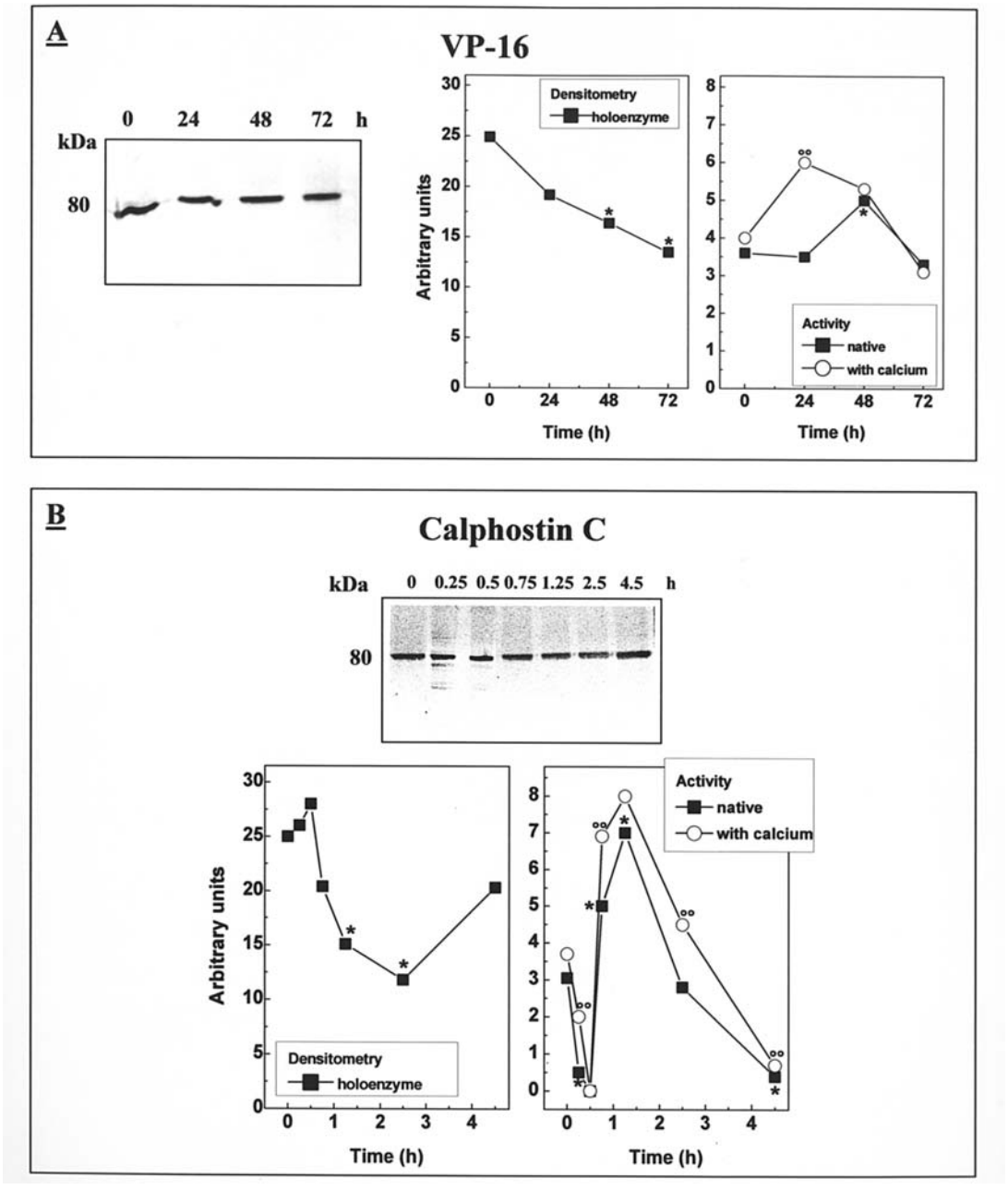

Figure 4. Cytosolic (CS) fraction. Both VP-16 (A) and calphostin C (B) lessen the levels of PKC-ß$_I$ holoenzyme but elicit delayed increases in immunoprecipitable PKC-ß$_I$-specific activities in the CS (cytosol) fraction of pyF111 cells. Cells were treated with either 1.0 μg ml^{-1} VP-16 or 75 nM calphostin C, sampled, and their CS fraction isolated; other experimental procedures were as for Fig. 2. The typical immunoblots and the points on the densitometric and specific activity curves are from at least four distinct experiments carried out with each apoptogen in triplicate. No CF-ß$_I$ moieties were detected in the CS. SEMs, not shown, were within ±11% the corresponding mean values. $^*p<0.05$ with respect to 0-h values; °°, $p<0.05$ with respect to values of corresponding time points.

thereafter falling back to below starting levels (Fig. 4A). However, adding calcium to the assay mixture increased the immunoprecipitable activity by as much as 52% ($p<0.01$) only at 24 h (Fig. 4A).

Calphostin C. After the first 30 min the PKC-ß$_I$ holoenzyme level started falling reaching its lowest level at 2.5 h (-53%, $p<0.01$) to increase again thereafter (48 h: -18%, p not significant vs. 0-h values). As with VP-16-treated cells, there were no detectable CFs at any time point (Fig. 4A and B). During the first 30 min, while the calphostin C was being photoactivated and the holoenzyme levels did not change, the immunoprecipitable enzymatic activity disappeared; hence, PKC-ß$_I$ was inactivated (Fig. 4B). Of course, this should have been expected from activating a protein kinase C inhibitor such as calphostin C. However, the inactive PKC-ß$_I$ molecules recovered rapidly thereafter and, surprisingly, the immunoprecipitable PKC-ß$_I$ activity surged dramatically upwards between 30 and 75 min to two-fold its '0'-h level ($p<0.001$) notwithstanding the concurrent fall in holoenzyme moieties, to finally collapse by 4.5 h as the cells were dying and evidently inactive holoenzymes were returned to the cytosol. A sizeable calcium-inducible activity was detectable at 0.25 h (+150%, $p<0.001$), 0.75 h (+37%, $p<0.05$) and 2.5 h (+50%, $p<0.01$) (Fig. 4B).

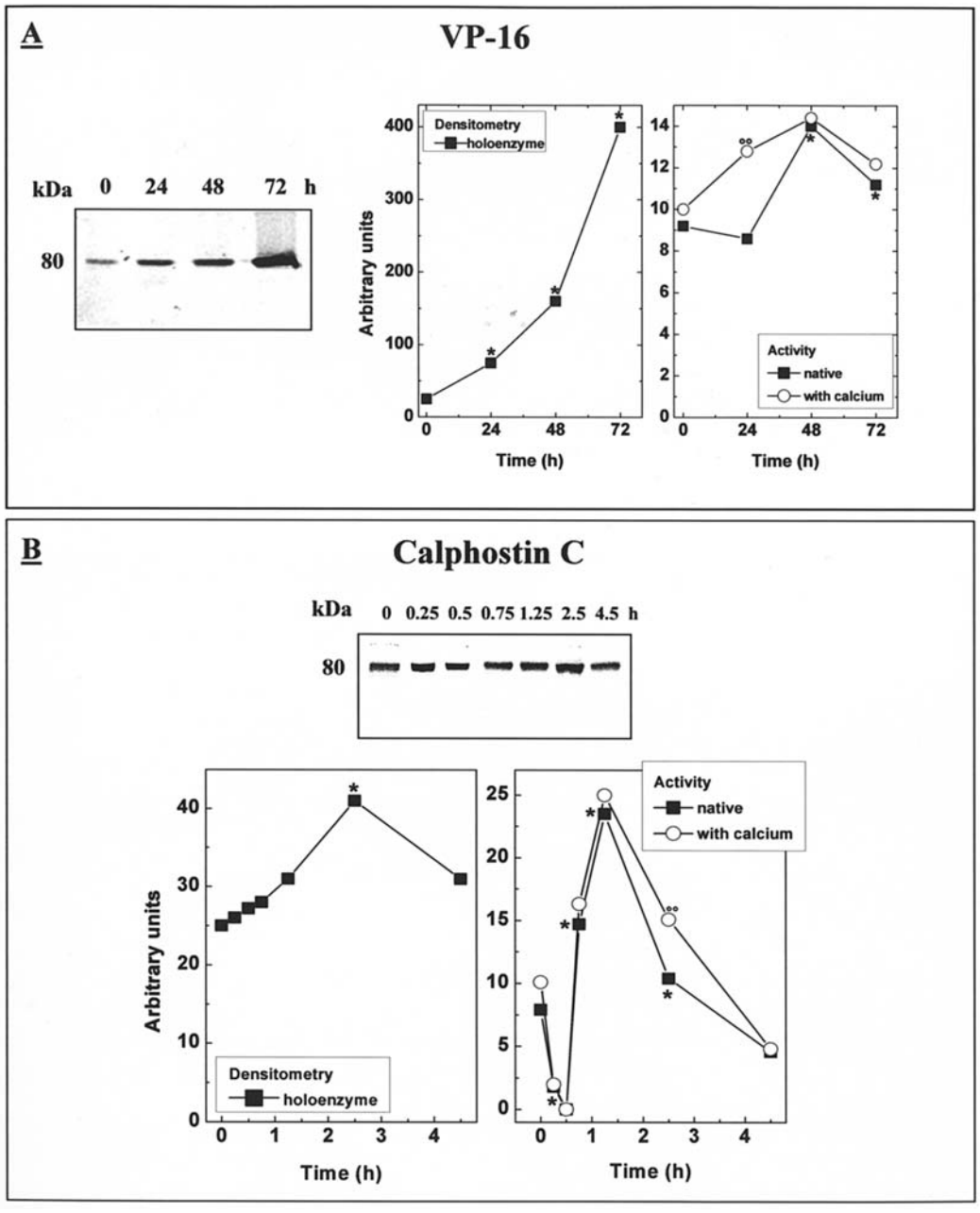

Figure 5. Cytoplasmic particulate (CP) fraction. Both VP-16 (A) and calphostin C (B) elicit the translocation of PKC-ß$_I$ holoenzyme and trigger delayed upsurges of immunoprecipitable PKC-ß$_I$-specific activities in CP (cytoplasmic particulate) fraction of pyF111 cells. Cells were treated with either 1.0 μg ml^{-1} VP-16 or 75 nM calphostin C, sampled, and their CP fraction isolated; other experimental procedures were as for Fig. 2. The representative immunoblots and the points on the densitometric and specific activity curves are from at least four different experiments carried out with each apoptogen in triplicate. No CF-ß$_I$ was detectable in the CP. SEMs, not shown, were within ±12% the corresponding mean values. *p<0.05 with respect to 0-h values; °°, p<0.02 with respect to the values of the corresponding time points.

CP (cytoplasmic particulate) fraction. The PKC-ß$_I$ holoenzyme, but not its CF, was also in the CP fraction associated with an immunoprecipitable activity that could not be increased by adding calcium (Fig. 5A and B).

VP-16. The holoenzyme was massively translocated to the CP fraction, where it accumulated in great amounts as it increased 3-fold by 24 h, 7-fold by 48 h and 17-fold by 72 h (p<0.001 at each time point) (Fig. 5A). Yet, there were no CFs. However, the immunoprecipitable native activity rose only by +63% (p<0.001) between 24 and 48 h, and then began dropping; clearly, most of the translocated holoenzyme moieties were inactive or rapidly inactivated. Adding calcium to the assay mixtures further increased the immunoprecipitable activity by 51% (p<0.02) only at 24 h as in the CS fraction (Fig. 5A).

Calphostin C. The PKC-ß$_I$ holoenzyme rose 64% (p<0.001) between 0 and 2.5 h then dropped (Fig. 5B). As occurred in the CS fraction (Fig. 4B), the rising holoenzyme was inactivated and the immunoprecipitable PKC-ß$_I$ activity vanished during the first 30 min while the calphostin C was being photoactivated. Then again as in the CS fraction, the PKC-ß$_I$ holoenzymes recovered when the illumination stopped and the immunoprecipitable activity surged dramatically to 3.2-fold the 0-h value (p<0.001) by 1.25 h, but then again

dropped below the starting value by 4.5 h as the cells were dying. Except for a significant rise at 2.5 h (+41%, $p<0.02$), there was no Ca^{2+}-inducible kinase activity (Fig. 5B).

Discussion

VP-16 and calphostin C trigger apoptosis differently in polyomavirus-transformed pyF111 cells (26-28). VP-16-treated cells take as long as one day just to start the apoptotic execution phase and then a further one to two days to die, while calphostin C-treated cells start the execution phase in only minutes and are dead by 6 h. Evidently, there is some common triggering event(s) that happens at different times in the two cases. Could PKC-$ß_I$, like its PKC$ß_{II}$ 'sibling' (28), somehow be involved in driving the cells along different paths to a common apoptotic death?

The PKC-$ß_I$ holoenzyme exists in all of the main compartments, particularly the NP and CS fractions, of the pyF111 rat fibroblasts, but its 47-kDa CF is found only in the NM fraction. The kinase is also active in all of the main fractions with the highest level of activity being in the NP followed by the NM where it collects after exposure to VP-16. We do not know the PKC-$ß_I$ substrates in pyF111 cells. Nor do we know why PKC-$ß_I$ is cleaved into its 47-kDa CF only in the NM fraction, where VP-16-treated pyF111 cells also put PKC-$ß_{II}$ and PKC-δ and cleave them into their CFs (26-28). However, unlike PKC-$ß_{II}$ and PKC-δ, PKC-$ß_I$ does not complex with and help drive the destruction of nuclear envelope-associated lamin B1 as does PKC-$ß_{II}$ in the VP-16-treated pyF111 cells (28).

The translocation and attachment of various PKCs to the nuclear membrane and cytoplasmic particulate (CP) components are parts of their activation mechanisms (34). The nuclear membrane-attached holoenzymes are activated by intracellular Ca^{2+} surges and lipid messengers cut out of membrane phospholipids by signal-activated membrane-associated phospholipases (35). The CFs in the nuclear membrane are constitutively activated when the holoenzyme N-terminal regulatory domains are chopped off at their 'hinge regions' by proteases such as neutral calpains I and II (36). Phosphorylation of proteins by the PKC holoenzymes and their CFs on either side of the nuclear membrane are believed to affect: i) the transport of gene transcription factors into the nucleus (37); ii) the activity of enzymes such as topoisomerase-II, which is part of the nuclear scaffold and is involved in chromosome condensation at prophase and chromosome separation at anaphase (29); iii) the breakdown of lamin B1 during apoptosis (28); and iv) the activities of chromatin associated with the NM and the lamin network (28,38).

The high basal levels of PKC-$ß_I$ activity in the nuclear envelopes of control ('0'-time) cells suggest that this kinase contributes both to the survival and proliferation of pyF111 fibroblasts. The increases in PKC-$ß_I$ activity at the NM caused by VP-16 and the lack of response to calphostin C at the NM could somehow be respectively linked to the DNA damage induced by the topoisomerase-II inhibitor, and to cytoplasmic activities being primarily caused by singlet oxygen and other reactive oxygen species generated during the 30-min photoactivation of calphostin C (39,40). However, not all PKC isoforms at the NM are activated by VP-16: PKC-δ activity undergoes an early, dramatic and persistent decline in VP-16-treated cells while also undergoing virtually no changes in calphostin C-exposed cells (26,27). Thus, the opposite VP-16-induced changes of PKC-$ß_I$ and PKC-δ underscore the complexity of the various PKC isoform-related responses to this same DNA-damaging agent at the NM.

The presence and very high basal activity of the PKC-$ß_I$ holoenzyme in the nucleoplasm (NP) of untreated pyF111 cells is in keeping with reports of it being involved in modulating gene expression (41,42) and fibroblast proliferation (10). By contrast, PKC-$ß_I$'s 'sibling' PKC-$ß_{II}$ does not get into the nucleoplasm (28) and only active PKC-δ CFs are found there (26,27). Although the times of onset of the increases in nucleoplasmic PKC-$ß_I$ activity in the pyF111 cells differ widely according to the apoptogen [1440 min (24 h) in VP-16-treated cells; 30-45 min in calphostin C-treated cells], in both cases they appear to coincide with the actual onset of the execution phase of apoptosis. Similarly, the later decline in PKC-$ß_I$ activity seem to be linked to the late stages of apoptosis execution and death of the cells. Thus, PKC-$ß_I$ signalling may be involved in starting the execution phase. However, a role for a PKC in calphostin C action would seem to be unlikely because of calphostin C being a PKC inhibitor. The answer to this apparent contradiction could lie in a surprising consequence of the initial 30-min photoactivation of calphostin C on PKC-$ß_I$ activity. Both VP-16 and calphostin C decreased the actual amounts of cytosolic holoenzyme moieties, which were translocated onto nuclear and/or cytoplasmic membranes. However, products generated during calphostin C's photoactivation inactivated the cytosolic (CS) and cytoplasmic particulate (CP) fraction PKC-$ß_I$. When the photoactivation was finished and the light was turned off, the CS- and CP-bound PKC-$ß_I$ recovered with a large, sharp overshoot of activity. i.e., photoactivation products had actually resulted in a net stimulation of PKC-$ß_I$ activity despite the continuing presence of a now-activated calphostin C.

The cytoplasm harbours cytochrome *c*, a potential apoptosis trigger. We have shown that the topoisomerase II-inhibiting mitosis-blocking VP-16 abruptly stops pyF111 cells from proliferating (26-28) and causes cytochrome *c* to spill out of their mitochondria into the cytosol during the first hour of treatment (26,27). This apoptogenesis-triggering early release of mitochondrial cytochrome *c* happens long before the activation of the lethal downstream caspases such as caspase-3. By briefly (30 min) inhibiting cytoplasmic PKC-$ß_I$ activity, calphostin C also causes a Bax-induced caspase-3-activating release of cytochrome *c* from mitochondria (43), but it works much faster than VP-16. Both apoptogens also cause the PKC-$ß_I$ holoenzyme to load into the CP fraction: the VP-16-elicited build-up is large, while the calphostin C-induced loading is smaller, given the much shorter survival time allowed by this apoptogen, but around 2.8 times faster than VP-16's. Though with different timings, a fraction of the PKC-$ß_I$ translocated onto the CP fraction was active, and the phosphorylation of a CP component(s) by the PKC-$ß_I$ may be part of a common cytochrome *c*/caspase-induced apoptotic trigger mechanism. However, the phosphorylation of this critical CP component by PKC-$ß_I$ in

ostin C-treated cells would have to occur during the post-calphostin C-photoactivation burst of activity. The importance of this CP fraction is further suggested by the fact that both VP-16 and calphostin C also loaded it with the PKC-ß$_I$ holoenzyme and increased its activity there (27).

The present results are the first indication, to our knowledge, that the ways by which PKC-ß$_I$ signalling is involved in apoptosis, just like PKC-δ signalling (26-28), depend on the mechanism(s) of action of the particular type of apoptogen. Thus, agents such as VP-16 that damage DNA influence PKC isoform signalling at the NM and NP fraction differently from calphostin C that acts primarily in the cytoplasm. The similarity of the shifts of PKC-ß$_I$ and PKC-δ in the CP fraction induced by these very different apoptogens points to this fraction being the likely site of a common apoptogenesis starter. We should investigate which proteins associate with PKC-ß$_I$ and PKC-δ forming specific signalling complexes or packets (44), and which substrates each PKC isoform phosphorylates in the subcellular fractions, especially the CP fraction, of untreated and of apoptosing fibroblasts, and whether these phosphorylations are involved in starting and driving apoptosis. Therefore, the present study is a necessary preliminary step for further investigations to be carried out by methods of functional proteomics (45).

In conclusion, the results of our previous (26-28) and present experiments suggest that the pattern of activation and inhibition of PKC isoforms in the various subcellular fractions depends on the apoptogenic agent in polyomavirus-transformed rat fibroblasts. This indicates significant differences in the substrates phosphorylated by PKCs and their active CFs in the various cellular fractions that nevertheless have the same end-point, apoptotic death. Hence, both the cell type and the apoptogen must be considered in order to adequately understand the roles of PKC signalling in drug-induced apoptosis.

Acknowledgements

This study was supported by research grants from the Ministry for Instruction, University and Research (M.I.U.R., Rome, 40 and 60% allotment funds).

References

1. Wetsel WC, Khan WA, Merchenthaler I, Rivera H, Halpern AE, Phung HM, Negro-Vilar A and Hannun YA: Tissue and cellular distribution of the extended family of protein kinase C isoenzymes. J Cell Biol 117: 121-133, 1992.
2. Housey GM, Johnson MD, Hsiao WL, O'Brian CA, Murphy JP, Kirschmeier P and Weinstein IB: Structural and functional studies of protein kinase C. Adv Exp Med Biol 234: 127-140, 1988.
3. Whitfield JF, Isaacs RJ, Jouishomme H, MacLean S, Chakravarthy BR, Morley P, Barisoni D, Regalia E and Armato U: C-terminal fragment of parathyroid hormone-related protein, PTHrP-(107-111), stimulates membrane-associated protein kinase C activity and modulates the proliferation of human and murine skin keratinocytes. J Cell Physiol 166: 1-11, 1996.
4. Ono Y, Kikkawa U, Ogita K, Fujii T, Kurokawa T, Asaoka Y, Sekiguchi K, Ase K, Igarashi K and Nishizuka Y: The expression and properties of two types of protein kinase C: alternative splicing from a single gene. Science 236: 1116-1120, 1987.
5. Kawakami Y, Kitaura J, Hartman SE, Lowell CA, Siraganian RP and Kawakami T: Regulation of protein kinase C beta I by two protein-tyrosine kinases, Btk and Syk. Proc Natl Acad Sci USA 97: 7423-7428, 2000.
6. Zhang J, Wang L, Petrin J, Bishop WR and Bond RW: Characterization of site-specific mutants altered at protein kinase C beta 1 isozyme autophosphorylation sites. Proc Natl Acad Sci USA 90: 6130-6134, 1993.
7. Keranen LM and Newton AC: Ca^{2+} differentially regulates conventional protein kinase Cs' membrane interaction and activation. J Biol Chem 272: 25959-25967, 1997.
8. Blobe GC, Stribling DS, Fabbro D, Stabel S and Hannun YA: Protein kinase C beta II specifically binds to and is activated by F-actin. J Biol Chem 271: 15823-15830, 1996.
9. Deacon EM, Pongracz J, Griffiths G and Lord JM: Isoenzymes of protein kinase C: differential involvement in apoptosis and pathogenesis. Mol Pathol 50: 124-131, 1997.
10. Umar S, Sellin JH and Morris AP: Increased nuclear translocation of catalytically active PKC-zeta during mouse colonocyte hyperproliferation. Am J Physiol Gastrointest Liver Physiol 278: G765-G774, 2000.
11. Bastiaens PI and Jovin TM: Microspectroscopic imaging tracks the intracellular processing of a signal transduction protein: fluorescent-labeled protein kinase C beta I. Proc Natl Acad Sci USA 93: 8407-8412, 1996.
12. Borner C, Ueffing M, Jaken S, Parker PJ and Weinstein IB: Two closely related isoforms of protein kinase C produce reciprocal effects on the growth of rat fibroblasts. Possible molecular mechanisms. J Biol Chem 270: 78-86, 1995.
13. Housey GM, Johnson MD, Hsiao WL, O'Brian CA, Murphy JP, Kirschmeier P and Weinstein IB: Overproduction of protein kinase C causes disordered growth control in rat fibroblasts. Cell 52: 343-354, 1988.
14. Svensson K, Zeidman R, Trollér U, Schultz A and Larsson C: Protein kinase C beta1 is implicated in the regulation of neuroblastoma cell growth and proliferation. Cell Growth Differ 11: 641-648, 2000.
15. Sauma S, Yan Z, Ohno S and Friedman E: Protein kinase C beta 1 and protein kinase C beta 2 activate p57 mitogen-activated protein kinase and block differentiation in colon carcinoma cells. Cell Growth Differ 7: 587-594, 1996.
16. Tonetti DA, Henning-Chubb C, Yamanishi DT and Huberman E: Protein kinase C-beta is required for macrophage differentiation of human HL-60 leukemia cells. J Biol Chem 269: 23230-23235, 1994.
17. Dieter P and Schwende H: Protein kinase C-alpha and -beta play antagonistic roles in the differentiation process of THP-1 cells. Cell Signal 12: 297-302, 2000.
18. O'Driscoll KR, Madden PV, Christiansen KM, Viage A, Slaga TJ, Fabbro D, Powell CT and Weinstein IB: Overexpression of protein kinase C beta I in a murine keratinocyte cell line produces effects on cellular growth, morphology and differentiation. Cancer Lett 83: 249-259, 1994.
19. Goldstein DR, Cacace AM and Weinstein IB: Overexpression of protein kinase C beta 1 in the SW480 colon cancer cell line causes growth suppression. Carcinogenesis 16: 1121-1126, 1995.
20. Zhu GH, Wong BC, Slosberg ED, Eggo MC, Ching CK, Yuen ST, Lai KC, Soh JW, Weinstein IB and Lam SK: Overexpression of protein kinase C-beta1 isoenzyme suppresses indomethacin-induced apoptosis in gastric epithelial cells. Gastroenterology 118: 507-514, 2000.
21. Cao MY, Shinjo F, Heinrichs S, Soh JW, Jongstra-Bilen J and Jongstra J: Inhibition of anti-IgM-induced translocation of protein kinase C beta I inhibits ERK2 activation and increases apoptosis. J Biol Chem 276: 24506-24510, 2001.
22. Pongracz J, Tuffley W, Johnson GD, Deacon EM, Burnett D, Stockley R and Lord JM: Changes in protein kinase C isoenzyme expression associated with apoptosis in U937 myelomonocytic cells. Exp Cell Res 218: 430-438, 1995.
23. MacFarlane DE and Manzel L: Activation of beta-isozyme of protein kinase C (PKC beta) is necessary and sufficient for phorbol ester-induced differentiation of HL-60 promyelocytes. Studies with PKC beta-defective PET mutant. J Biol Chem 269: 4327-4331, 1994.
24. Laouar A, Glesne D and Huberman E: Involvement of protein kinase C-beta and ceramide in tumor necrosis factor-alpha-induced but not Fas-induced apoptosis of human myeloid leukemia cells. J Biol Chem 274: 23526-23534, 1999.
25. Raptis L, Lamfrom H and Benjamin TL: Regulation of cellular phenotype and expression of polyomavirus middle T antigen in rat fibroblasts. Mol Cell Biol 5: 2476-2485, 1985.

26. Dal Pra I, Whitfield JF, Chiarini A and Armato U: Changes in nuclear protein kinase C-delta holoenzyme, its catalytic fragments, and its activity in polyomavirus-transformed pyF111 rat fibroblasts while proliferating and following exposure to apoptogenic topoisomerase-II inhibitors. Exp Cell Res 249: 147-160, 1999.
27. Dal Pra I, Whitfield JF, Chiarini A and Armato U: Increased activity of the protein kinase C-delta holoenzyme in the cytoplasmic particulate fraction precedes the activation of caspases in polyomavirus-transformed pyF111 rat fibroblasts exposed to calphostin C or topoisomerase-II inhibitors. Exp Cell Res 255: 171-183, 2000.
28. Chiarini A, Whitfield JF, Armato U and Dal Pra I: Protein kinase C-beta II is an apoptotic lamin kinase in polyomavirus-transformed, etoposide-treated pyF111 rat fibroblasts. J Biol Chem 277: 18827-18839, 2002.
29. Fortune JM and Osherhoff N: Topoisomerase II as a target for anticancer drugs: when enzymes stop being nice. Prog Nucleic Acid Res Mol Biol 64: 221-253, 2000.
30. Sciorra VA, Hammond SM and Morris AJ: Potent direct inhibition of mammalian phospholipase D isoenzymes by calphostin-C. Biochemistry 40: 2640-2646, 2001.
31. Amarante-Mendez GP, Finucane D and Green DR: Cells, a Laboratory Manual. Spector Dl, Goldman RD and Leinwald LA (eds). Vol. 1, Cold Spring Harbor Laboratory Press, pp15.6-15.7, 1998.
32. McIntosh CHS and Plummer DT: The subcellular localization of acetylcholinesterase and its molecular forms in pig cerebral cortex. J Neurochem 27: 449-457, 1976.
33. Bradford MM: A rapid and sensitive method for the quantitation of microgram quantities of protein utilizing the principle of protein-dye binding. Anal Biochem 72: 248-254, 1976.
34. Hocevar BA and Fields AP: Selective translocation of beta II-protein kinase C to the nucleus of human promyelocytic (HL60) leukemia cells. J Biol Chem 266: 28-33, 1991.
35. Kochs G, Hummel R, Fiebich B, Sarre TF, Marme D and Hug H: Activation of purified human protein kinase C alpha and beta I isoenzymes *in vitro* by Ca^{2+}, phosphatidylinositol and phosphatidylinositol 4,5-bisphosphate. Biochem J 291: 627-633, 1993.
36. Mizuno K, Noda K, Araki T, Imaoka T, Kobayash Y, Akita Y, Shimonaka M, Kishi S and Ohno S: The proteolytic cleavage of protein kinase C isotypes, which generates kinase and regulatory fragments, correlates with Fas-mediated and 12-O-tetradecanoyl-phorbol-13-acetate-induced apoptosis. Eur J Biochem 250: 7-18, 1997.
37. Ventura C and Maioli M: Protein kinase C control of gene expression. Crit Rev Eukaryot Gene Expr 11: 243-267, 2001.
38. Beckmann R, Buchner K, Jungblu PR, Eckerskorn C, Weise C, Hilbert R and Hucho F: Nuclear substrates of protein kinase C. Eur J Biochem 210: 45-51, 1992.
39. Wang SS, Mathes C and Thompson SH: Membrane toxicity of the protein kinase C inhibitor calphostin A by a free-radical mechanism. Neurosci Lett 157: 25-28, 1993.
40. Diwu Z and Lown JW: Photosensitization with anticancer agents 19. EPR studies of photodynamic action of calphostin C: formation of semiquinone radical and activated oxygen on illumination with visible light. Free Radic Biol Med 16: 645-652, 1994.
41. Chen CC, Wang JK and Lin SB: Antisense oligonucleotides targeting protein kinase C-alpha, -beta I, or -delta but not -eta inhibit lipopolysaccharide-induced nitric oxide synthase expression in RAW-264.7 macrophages: involvement of a nuclear factor kappa B-dependent mechanism. J Immunol 161: 6206-6214, 1998.
42. Koya D, Jirousek MR, Lin YW, Ishii H, Kuboki K and King GL: Characterization of protein kinase C beta isoform activation on the gene expression of transforming growth factor-beta, extracellular matrix components, and prostanoids in the glomeruli of diabetic rats. J Clin Invest 100: 115-126, 1997.
43. Ikemoto H, Tani E, Ozaki I, Kitagawa H and Arita N: Calphostin C-mediated translocation and integration of Bax into mitochondria induces cytochrome c release before mitochondrial dysfunction. Cell Death Differ 7: 511-520, 2000.
44. Ping P, Zhang J, Pierce Jr WM and Bolli R: Functional proteomic analysis of protein kinase C ε signalling complexes in the normal heart and during cardioprotection. Circ Res 88: 59-62, 2001.
45. Zhang J, Baines CP, Zong C, Cardwell EM, Wang G, Vondriska TM and Ping P: Functional proteomic analysis of a three-tier PKCepsilon-Akt-eNOS signaling module in cardiac protection. Am J Physiol Heart Circ Physiol 288: H954-H961, 2005.

SPANDIDOS PUBLICATIONS